PREDICTION OF MAGNETIZING CURRENTS IN POWER TRANSFORMERS USING NUMERICALLY SIMULATED OPEN -CIRCUIT TESTS

Antônio Flavio Licarião Nogueira[1], Gabriel Grunitzki Facchinello[2] & Leonardo Adriano Ramos[3]
[1,2,3] Santa Catarina State University, Joinville, Santa Catarina, Brazil

ABSTRACT
Numerical field solutions may be used to predict the magnetizing current waveform of power transformers for a giving value of sinusoidal voltage supply. This note concerns the sequence of operations necessary to estimate the magnetizing current waveform of power transformers employing a set of numerically simulated open-circuit tests.

Keywords: *Finite element analysis, Inductance, Magnetic cores, Power transformers.*

1. INTRODUCTION
When the primary winding of an unloaded transformer is energized, it may draw a high magnitude transient current from the supply. This almost entirely unidirectional inrush current rises abruptly to its maximum value in the first half-cycle and henceforth decays exponentially until the steady-state magnetizing conditions are reached [1], [2]. The present study introduces the sequence of operations necessary to evaluate the nonsinusoidal steady-state magnetizing current of power transformers by means of numerically simulated open-circuit tests.
In the open-circuit test, the transformer's primary winding is supplied with rated voltage, and the secondary winding is left open-circuited. At this operating condition, saturation levels are sufficiently high to cause the magnetizing current to contain a significant proportion of harmonics. In other words, the operating condition involves sinusoidal applied voltage but nonsinusoidal current due to the nonlinear behavior of the primary winding inductance [3].
The test problem considered in the present study concerns the evaluation of the magnetizing current of the idealized single-phase shell-type transformer described in [4]. A study reporting on the behavior of this particular transformer under magnetically linear operation is presented in [5]. A key feature of the numerical model for predicting the magnetizing current waveshape is the use of a nonlinear magnetization characteristic for the transformer's magnetic core. In the present analysis, the homogeneous composite material, commercially known as "Carpenter Silicon Core Iron A, 1066C Anneal" is used to model all regions that form the transformer's magnetic core. The *B-H* curve for this composite material is presented in figure 1.

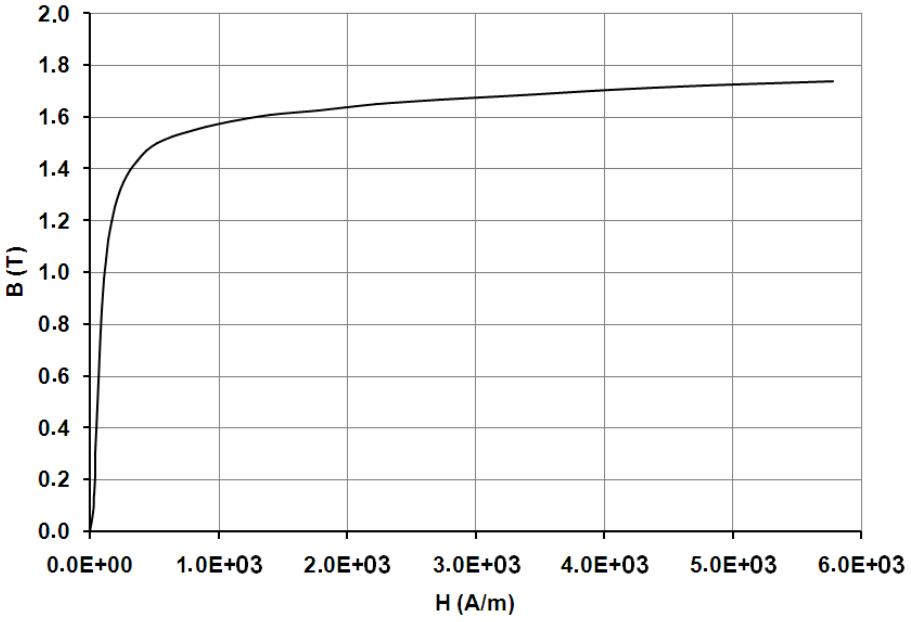

Figure 1. B-H curve for the composite material commercially known as "Carpenter Silicon Core Iron A, 1066C Anneal".

2. PROBLEM DESCRIPTION

The shell-type transformer under analysis consists of two concentric coils wound around the core's central limb. The secondary circuit is wound over the top of the primary. Both windings have equal numbers of turns, and N_1=N_2=1000. A cross sectional view of the transformer showing the core's geometry as well as the placement of the two windings appears in figure 2(a). Each coil is modeled by two non-contiguous rectangular regions, and the properties of these regions include the specification of the coil's number of turns and terminal current. In addition, each pair of regions representing a stranded coil must be defined as series-connected [6], [7]. The geometrical details of the device are indicated in figure 2(b), with the dimensions in meter.

The numerical model includes a layer of air that surrounds the transformer. The air layer terminates at the artificial, external boundary indicated in figure 2(a). Along the external boundary, the magnetic vector potential ***A*** is made equal to zero. This boundary condition is commonly referred to as a "Dirichlet boundary", and is used to close the domain of analysis. As indicated in figure 2(b), the depth or length of the model in the longitudinal or *z* direction is 0.6 m. The two-dimensional simulation software "finite element method magnetics" (FEMM) has been used to obtain the magnetostatic solutions [7]. This is a current-driven finite-element program that works with prescribed currents rather than voltages.

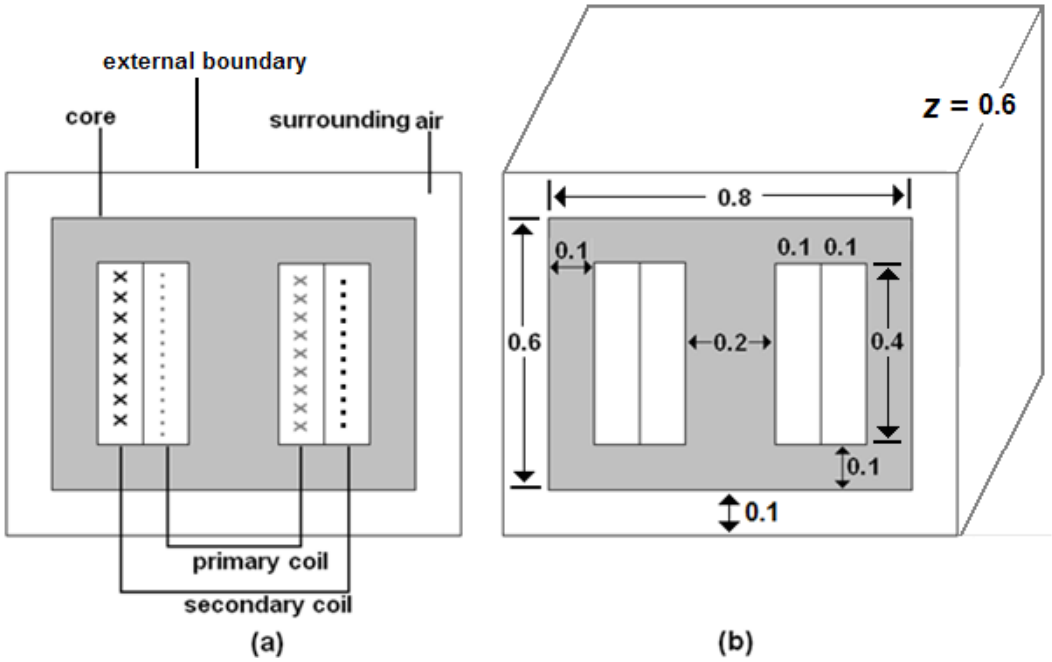

Figure 2. (a) Cross sectional view of the transformer's model; (b) Geometrical dimensions, in meter.

3. THE SIMULATION TECHNIQUE

A sequence of open-circuit tests can be simulated in a finite-element CAD system to produce an estimate for the magnetizing current waveshape for one particular value of terminal voltage. The procedure is described in [8] and [9]. Firstly, the range of instantaneous magnetizing currents, up to the largest peak current likely to be encountered, must be established. The set I_T of tabulated currents values is

$$I_T = \{i_k, k = 1,\ldots,N\}. \quad (1)$$

The set of tabulated instantaneous currents i_k ranging from zero up to the maximum value can be arbitrarily chosen, or analytical functions may be used to represent the increase of the instantaneous currents; usual choices include, for example, linear, exponential or sinusoidal variations. Open-circuit tests related to each of these currents are simulated and produce a set *A* of magnetic vector potential distributions $A_k(x,y)$,

$$A = \{A_k(x, y), k = 1,\ldots,N\}. \quad (2)$$

The primary flux linkages λ_k are computed for each potential solution A_k using the equation

$$\lambda_k = \frac{1}{i_k} \int_{S_p} AJdS, \tag{3}$$

where S_p denotes the cross-sectional area of the primary winding, and J denotes the current density in the winding regions. For each potential solution, the program FEMM automatically calculates the flux linkages of the primary winding as part of the circuit properties [7]. Every flux linkage λ_k corresponds to a specific current i_k, and the two sets taken together define a curve of flux linkages against current. This curve resembles a *B-H* curve.

It will be assumed that the primary terminal voltage *e(t)* for which the magnetizing current waveshape is being constructed is sinusoidal,

$$e(t) = E\cos(\omega t). \tag{4}$$

The flux linkages of the primary winding are also assumed to vary in a sinusoidal fashion,

$$\lambda(t) = -\frac{1}{\omega} E\sin(\omega t). \tag{5}$$

Assuming that hysteresis is absent, the magnetizing current exhibits quarter-cycle symmetry,

$$i(\omega t + \pi) = -i(\omega t). \tag{6}$$

In this case, it is possible during a quarter of the *ac* cycle to obtain the sequence of time instants t_k at which the computed flux linkages λ_k are reached,

$$t_k = -(1/\omega)\arcsin\left[-\omega\lambda_k \big/ E\right]. \tag{7}$$

It is worth noting that the parameter E in (7) represents the peak value of the sinusoidal exciting voltage for which the magnetizing current waveshape is to be obtained. The parameter E is computed for the maximum flux linkage, given by the field solution that represents the first peak value of current, i.e., at the angular position $\omega t=\pi/2$ rad. The set T of time values obtained from (7) is

$$T = \{t_k, k = 1,\ldots,N\}. \tag{8}$$

This set of time values corresponds to the set of tabulated current values I_T defined in equation (1) and is used to obtain the magnetizing current waveform.

4. NUMERICAL RESULTS

In order to predict the magnetizing current waveshape related to one particular value of terminal voltage, the starting point is the definition of the tabulated terminal currents. In the present analysis, the transformer's peak current at no-load operation is 2.0 A. It is assumed that the instantaneous, tabulated current *i(t)* rises sinusoidally from zero to 2.0 A, its peak value, over the first-quarter of the *ac* cycle,

$$i(t) = 2.0\sin(\omega t),\ 0 \langle \omega t \langle \pi/2. \tag{9}$$

In this particular example, the set of sixteen static solutions is used to define the curve shown in figure 3 that represents the variation of computed flux linkages against the tabulated terminal currents. In table 1, terminal currents are presented in column 3, and related flux linkages are presented in column 4, respectively.

Table 1. Specified and computed data to obtain the magnetizing current over a quarter cycle.

Sequence of operations	Specified data		Computed data	
	Angle ωt	Tabulated sinusoidal current	Flux linkages given by field solution	Angle ωt computed using eqn. (7)
	(degree)	(ampere)	(weber)	(degree)
	0	0	0	0
1	1.0	0.0349	6.46	2.38
2	2.0	0.0698	36.78	13.71
3	4.0	0.1395	84.44	32.96
4	6.0	0.2091	107.07	43.61
5	7.5	0.2610	116.57	48.67
6	15.0	0.5176	137.02	61.97
7	22.5	0.7653	144.40	68.47
8	30.0	1.0000	147.73	72.12
9	37.5	1.2175	150.01	75.11
10	45.0	1.4142	151.64	77.66
11	52.5	1.5867	152.97	80.21
12	60.0	1.7320	153.95	82.65
13	67.5	1.8477	154.57	84.73
14	75.0	1.9318	154.95	86.57
15	82.5	1.9828	155.16	88.30
16	90.00	2.0000	155.23	90.00

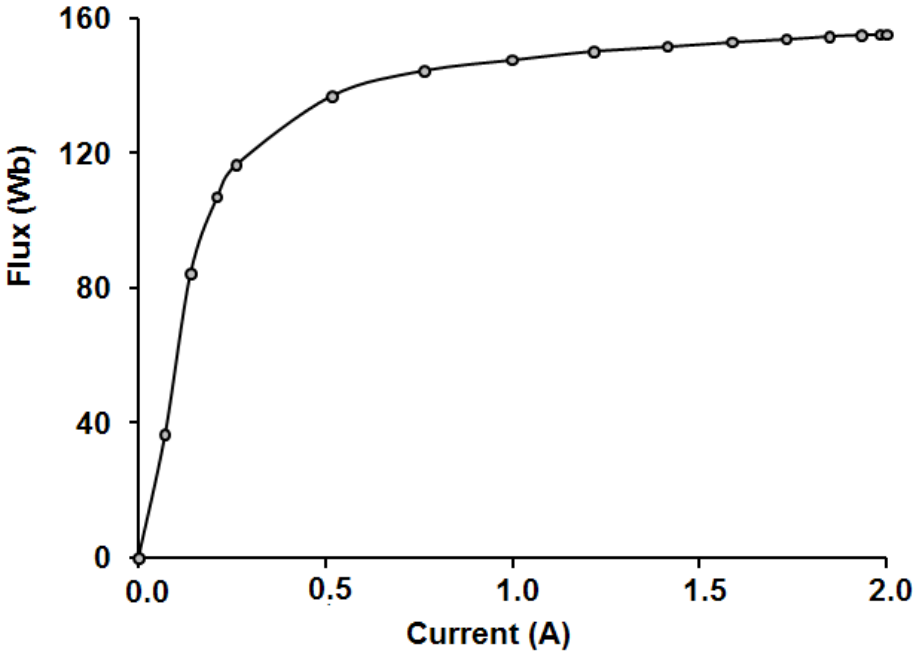

Figure 3. Variation of computed flux linkages against tabulated currents.

Equation (7) is employed to determine the sequence of time instants t_k at which the computed flux linkages indicated in column 4 of table 1 are reached during a quarter cycle. To obtain the sequence of angles indicated in column 5 of table 1, it is necessary to multiply each time instant t_k by the fundamental angular frequency $\omega=2\pi(60)$ rad/s. The curves representing the sinusoidal variation of tabulated currents together with instantaneous values of the distorted magnetizing current over the first-quarter of the *ac* cycle are presented in the graph of figure 4.

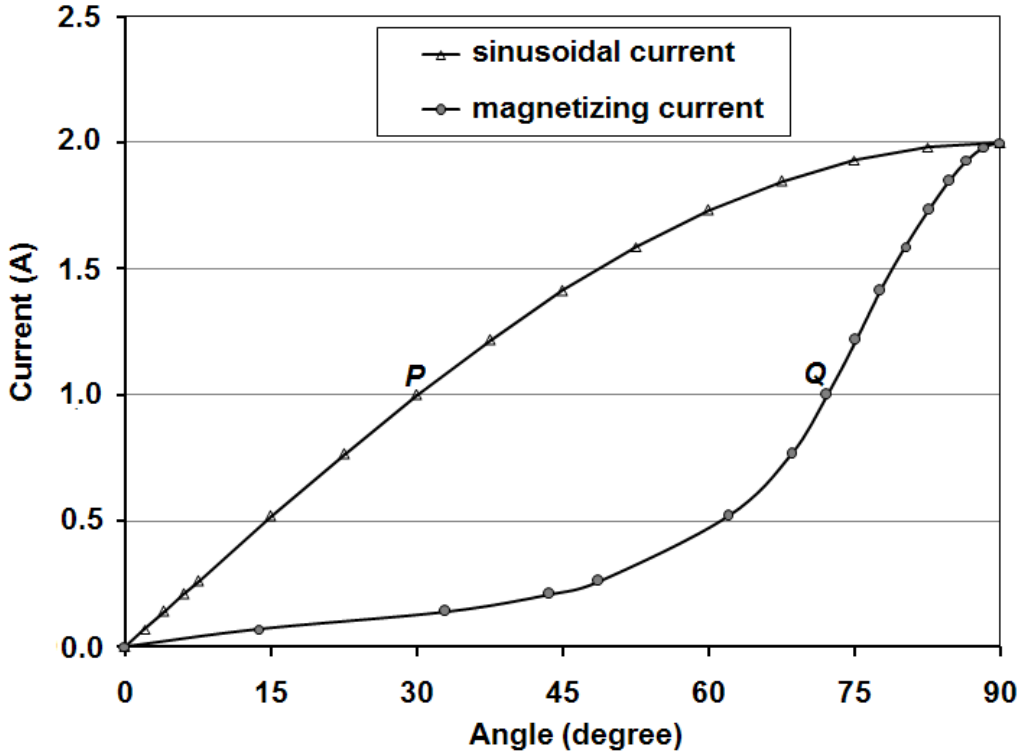

Figure 4. Terminal current over a quarter cycle: (Δ) *Sinusoidal variation;* (o) *Magnetizing current.*

With reference to the graph presented in figure 4, it is important to notice that, in this particular analysis, there are altogether seventeen data points belonging to each curve. Because the magnetizing current waveform begins at $i(0)=0$, only sixteen field solutions have been used to obtain the magnetizing current waveform over the first-quarter of the *ac* cycle.

A close observation of points *P* and *Q* indicated in the graph of figure 4 helps to explain the distorted shape of the magnetizing current waveform. Both points, *P* and *Q*, are related to the terminal current of 1.0 A, necessary to produce a linkage flux of 147.73 webers (see table 1, line 8). If the instantaneous current increase were truly sinusoidal, that particular flux linkage would be reached at time instant t=1.39 millisecond, which corresponds to 30 electrical degrees. In fact, that flux linkage, as computed by equation (7), is only reached later, at time instant t=3.34 milliseconds, which corresponds to 72.12 electrical degrees. This slower increase of the predicted magnetizing current is caused by the high levels of the transformer's inductance when operating at the non-saturated portion of the magnetization characteristic. It is important to notice that the steep slope of the *B*-*H* curve for small *H*-fields (and related driving currents) intrinsically represents a rapid increase in the primary winding inductance at the very beginning of the terminal current excursion, as shown in the curve exhibited in figure 5. Following its initial rapid increase, the inductance of the primary winding starts to decrease after its maximum value. However, inductance values remain sufficiently high to slow down the increase in current values until the terminal current reaches, say, 1.0 A, half of the first peak value.

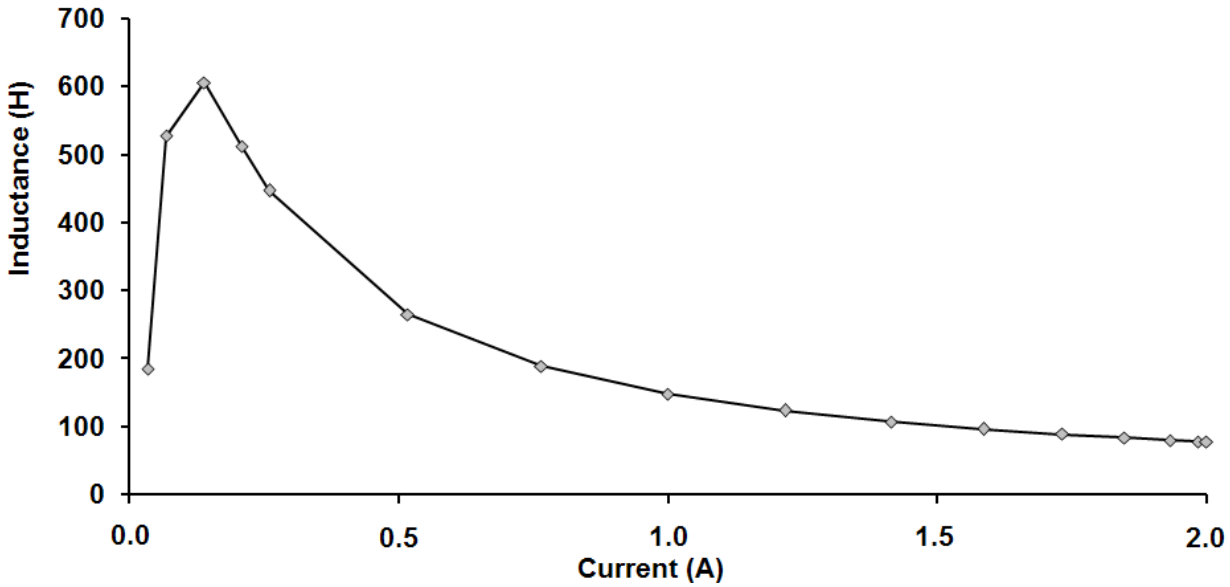

Figure 5. Variation of the primary winding inductance with increased terminal current.

The dash characteristic shown in the graph of figure 6 represents the magnetizing current waveform over the first-half of the *ac* cycle. The central portion of the waveform is highlighted by a solid curve marked with those circles that represent the magnetizing current estimates around the peak value. This waveform has been obtained by exploiting the quarter-cycle symmetry exhibited by the total magnetizing current waveform. The property of quarter-cycle symmetry exhibited by the magnetizing current waveform has two implications: (i) values of the magnetizing current *i* repeat at intervals of a quarter cycle; (ii) over the first-half of the *ac* cycle, the magnetizing current waveform is represented by a curve that is unimodal and symmetrical with respect to its maximum or peak value. The graph of figure 6 contains 33 data points altogether. Sixteen data points are situated to the left of the peak value. The remaining 16 data points situated to the right of the peak value have been obtained simply by enforcing the repeatability of the waveform over the second-quarter of the *ac* cycle.

An enlarged view of the central portion of the magnetizing current waveform is shown in the graph of figure 7. With the aid of this curve, it is possible to observe the repeatability of the magnetizing current values on both sides of the peak value i_k. If N denotes the number of data points over the first-quarter of the *ac* cycle $[0, \pi/2]$, up to the peak value, the data points over the second-quarter of the *ac* cycle $(\pi/2, \pi]$ are then obtained by enforcing the mathematical relationships,

$$\omega t_{k+1} = \pi - \omega t_{k-1}; k = 1,\ldots,N \quad (10)$$

and

$$i_{k+1} = i_{k-1}; k = 1,\ldots,N. \quad (11)$$

where ω represents the fundamental angular frequency.

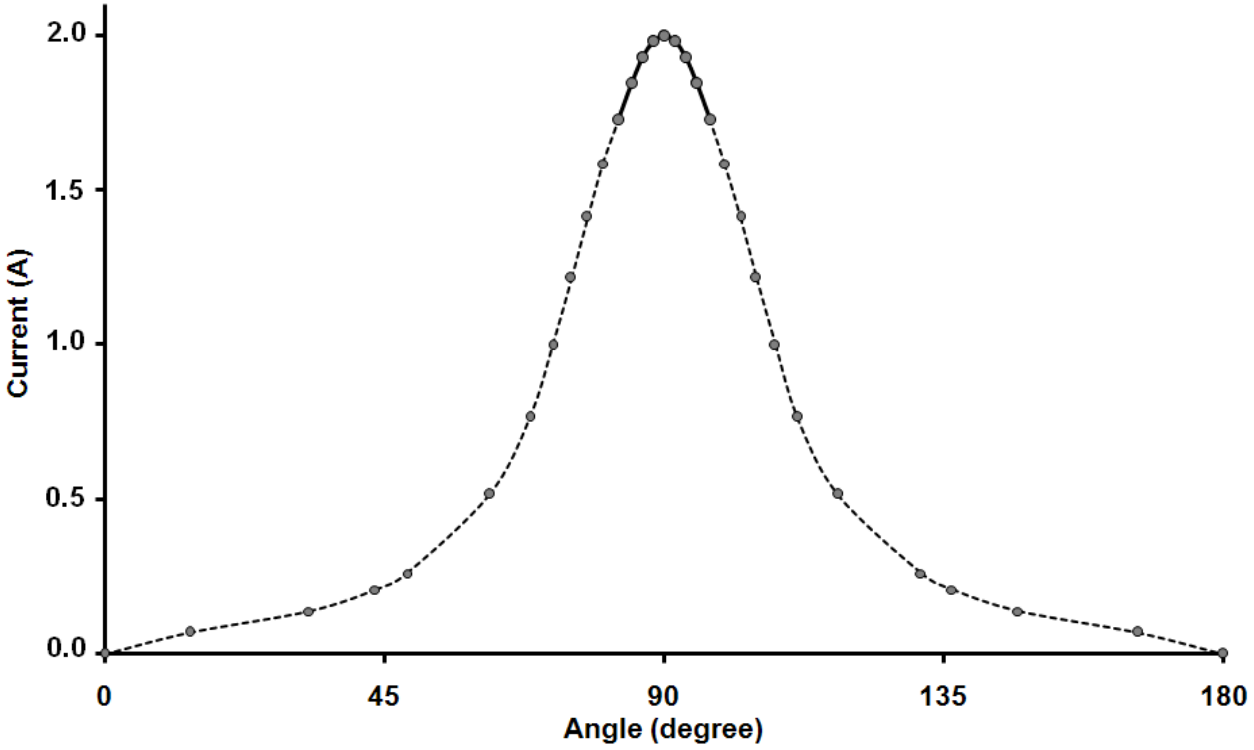

Figure 6. Instantaneous variation of the magnetizing current over the first-half of the ac cycle.

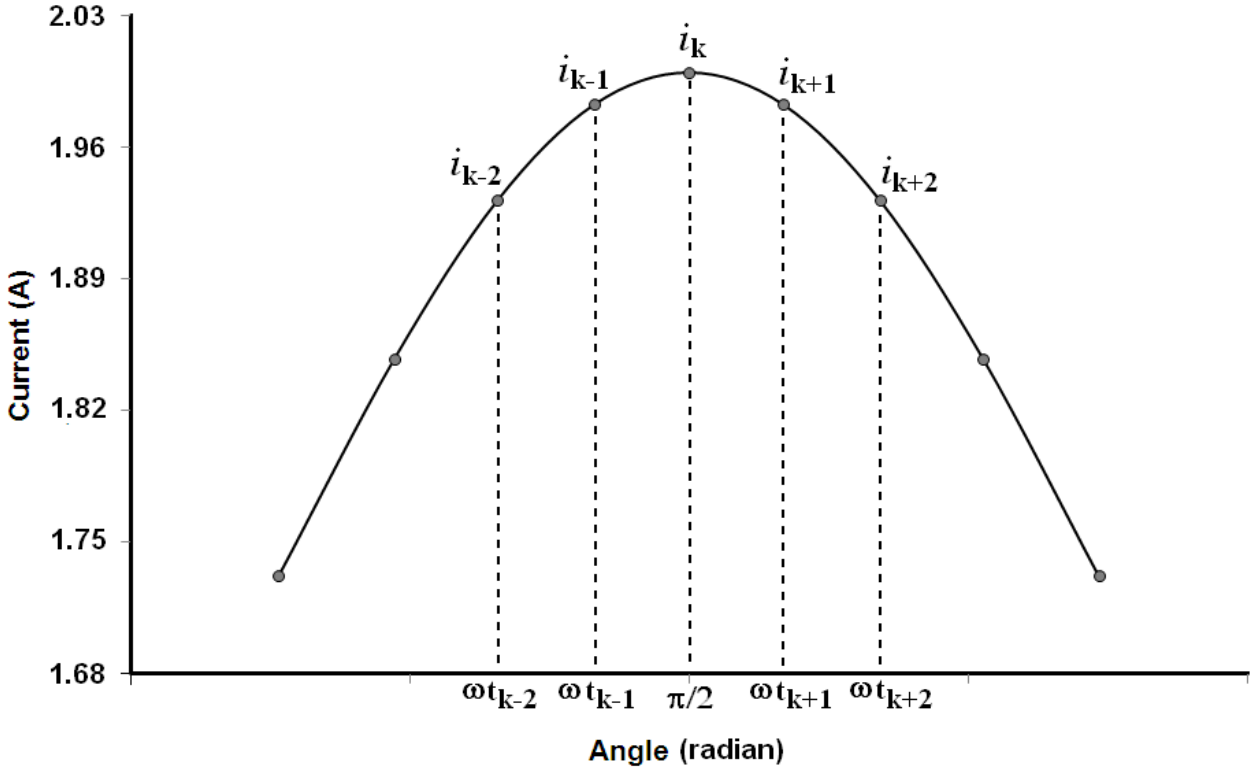

Figure 7. Enlarged view of the magnetizing current waveform around the first peak value.

The magnetizing current waveform over a full cycle [0, 2π] can be readily obtained by applying the mathematical relationship

$$i(\omega t + \pi) = -i(\omega t), \quad (6)$$

that enforces the quarter-cycle symmetry property of the total current waveform. The resulting magnetizing current waveform over a full *ac* cycle is shown in the graph of figure 8. This waveform represents the magnetizing current when the transformer is supplied by a sinusoidal primary voltage *e*(t) for which the peak value is *E*=58.52 kV. This is a steady-state periodic current, and the shape the current's waveform is in accordance with the physical understanding of the open-circuit operating condition. In the predicted waveform, one can observe a sequence of continuously changing slopes, representing the sequence of the transformer's unsaturated and saturated magnetizing conditions. Its peak value is 2.0 A, and the root-mean-square value is 0.79 A.

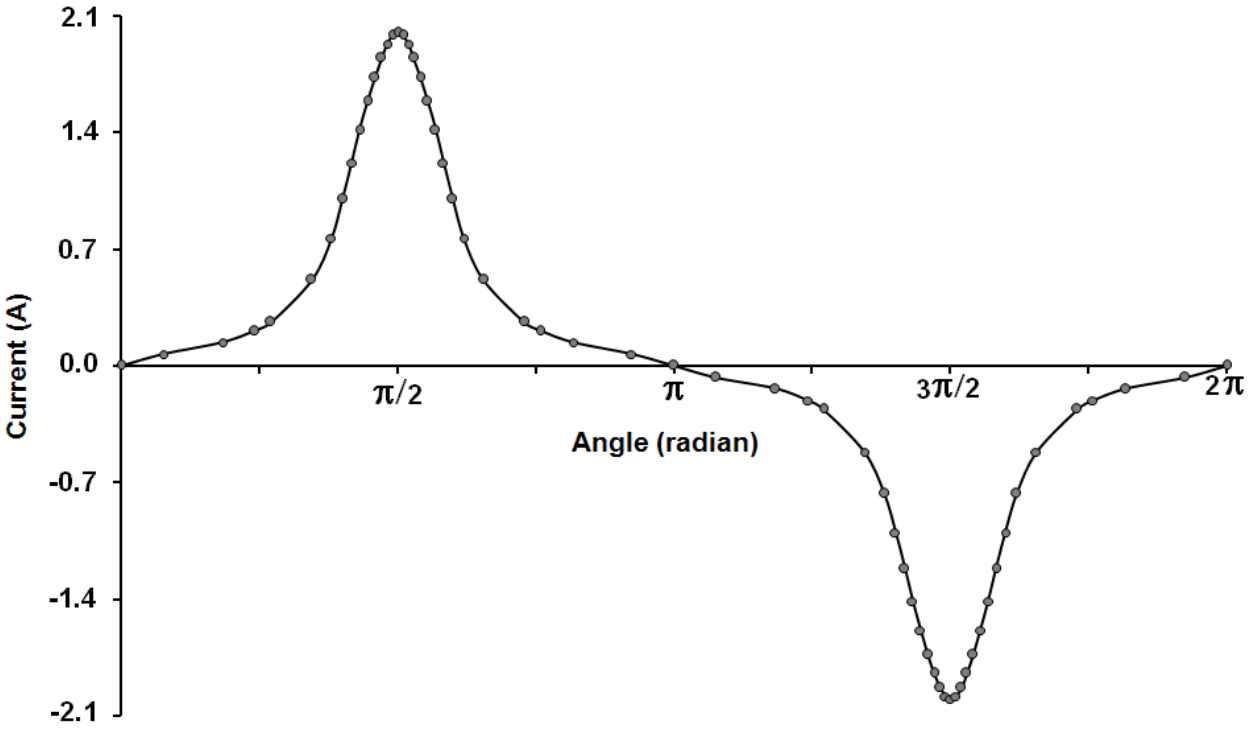

Figure 8. Magnetizing current over a full ac cycle.

In the several publications about the no-load operation of power transformers, it is usual to find tables containing information such as the magnitude of the magnetizing current fundamental-frequency component I_1 together with the percentage of the 3rd, 5th and 7th harmonics with respect to that fundamental component. The harmonic content of magnetizing currents is a quantity of considerable interest to transformer designers as well as to system engineers [9].

Information related to the transformer's magnetizing current waveform such as peak value, true root-mean-square (rms) value and total harmonic distortion (TDH) are useful to systems engineers when characterizing the power quality of electric power systems [10]. Rickley et al. have proposed a method for detection of faults in three-phase transformers based on measurements of the magnetizing current [11]. Luciano et al. have registered the increase in power transformers magnetizing currents over a period of thirteen years to inspect the effect of oxidation on the magnetic cores [12].

5. CONCLUSIONS

The note explains how to predict the magnetizing current of power transformers using numerically simulated open-circuit tests. The test problem concerns the evaluation of the magnetizing current of an idealized single-phase shell-type transformer, for a given value of sinusoidal voltage supply. A key feature of the numerical calculations for predicting the magnetizing current is the use of a nonlinear magnetization characteristic for the transformer's magnetic core. Once the magnetizing current waveform exhibits quarter-cycle symmetry, all finite element

calculations are related to the first-quarter of the *ac* cycle wherein the current rises from zero up to its first peak value. Based on the quarter-cycle symmetry of the expected waveform, simple mathematical relationships are applied and data points for the full *ac* cycle are readily obtained. The magnetizing current waveform of the transformer under investigation is in accordance with the physical understanding of the open-circuit operating condition, wherein the transformer behaves as a nonlinear reactor.

6. ACKNOWLEDGEMENT

The research group acknowledges the financial support, in the form of scholarships, from the Brazilian National Council of Technological and Scientific Development (CNPq). Thanks are given to David Meeker (dmeeker@ieee.org) for the use of the finite element CAD system *FEMM*. The authors also give thanks to the Brazilian Federal Agency for Postgraduate Studies (CAPES) for the sponsored access to several scientific web sites.

7. REFERENCES

[1] M. Khederzadeh, "Mitigation of the impact of transformer inrush current on voltage sag by TCSC", *Electric Power Systems Research*, doi:10.1016/j.epsr.2010.01.011

[2] Y. Wang and S.G. Abdulsalam, "Analytical formula to estimate the maximum inrush current", *IEEE Trans. on Power Delivery*, doi: 10.1109/TPWRD.2008.919153

[3] M. Jamali, M. Mirzaie, S. Asghar Gholamian, "Calculation and analysis of transformer inrush current based on parameters of transformer and operating conditions", *Electronics and electrical engineering*, Kaunas: Technologija, 2011. No. 3(109), pp. 17-20.

[4] J.D. Edwards, *An introduction to MagNet for static 2D modeling* (Infolytica Corporation, Montreal, 2007), pp. 62-67. Available:http://courses.ee.sun.ac.za/Energiestelsels_344/files/downloads/MagNet-Introduction.pdf

[5] A.F.L. Nogueira, "Calculation of power transformers equivalent circuit parameters using numerical field solutions", *International Journal of Research and Reviews in Applied Sciences*, vol. 17, No 1, October 2013.

[6] A.F.L. Nogueira and L.J.A.S. Maldonado, "Analysis of AC contactors combining electric circuits, time-harmonic finite element simulations and experimental work", *International Journal of Research and Reviews in Applied Sciences*, **14**(3) 513-525 (2013).

[7] D. Meeker, *Finite element method magnetics, user's manual*. Available: http://www.femm.info/Archives/doc/manual42.pdf

[8] P.P. Silvester and M.V.K. Chari, "Finite element solution of saturable magnetic field problems", *IEEE Transactions on Power Apparatus and Systems*, vol. PAS-89, no. 7, pp. 1642-1651, 1970.

[9] D.A. Lowther and P.P. Silvester, *Computer-aided design in magnetics*, Springer-Verlag, New York, 1986, pp. 183.

[10] A.H. Al-Haj and I. El-Amin, "Factors that influence transformer no-load current harmonics", *IEEE Trans. on Power Delivery*, vol. 15, no. 1, pp. 163-166, 2000.

[11] A.L. Rickley, R.E. Clark and E.H. Povey, "Field measurements of transformer excitation current as a diagnostic tool", *IEEE Trans. on Power Apparatus and Systems*, vol. PAS-100, no. 4, pp. 1985-1988, April 1981.

[12] B.A. Luciano, T.C. Batista, M.A.G. Camacho, R.C.S. Freire and W.B. De Castro, "Medições das perdas e da corrente de excitação em transformadores monofásicos de baixa potência com núcleo de liga amorfa: antes e depois do processo de oxidação", in *VIII Semetro*, João Pessoa, Brazil, June 2009. (In Portuguese)